

Non-Gaussian Error Distribution of ${}^7\text{Li}$ Abundance Measurements

Sara Crandall, Stephen Houston, and Bharat Ratra

*Department of Physics, Kansas State University, 116 Cardwell Hall, Manhattan, KS
66506, USA*

sara1990@phys.ksu.edu, stephen8@phys.ksu.edu, and ratra@phys.ksu.edu

ABSTRACT

We construct the error distribution of ${}^7\text{Li}$ abundance measurements for 66 observations (with error bars) used by Spite et al. (2012) that give $A(\text{Li}) = 2.21 \pm 0.065$ (median and 1σ symmetrized error). This error distribution is somewhat non-Gaussian, with larger probability in the tails than is predicted by a Gaussian distribution. The 95.4% confidence limits are 3.0σ in terms of the quoted errors. We fit the data to four commonly used distributions: Gaussian, Cauchy, Student's t , and double exponential with the center of the distribution found with both weighted mean and median statistics. It is reasonably well described by a widened $n = 8$ Student's t distribution. Assuming Gaussianity, the observed $A(\text{Li})$ is 6.5σ away from that expected from standard Big Bang nucleosynthesis given the *Planck* observations (Coc et al. 2014). Accounting for the non-Gaussianity of the observed $A(\text{Li})$ error distribution reduces the discrepancy to 4.9σ , which is still significant.

1. Introduction

Standard Big Bang nucleosynthesis (BBN) is used to model the production of light elements D, ${}^3\text{He}$, ${}^4\text{He}$, and ${}^7\text{Li}$ during the first 20 minutes of the development of the universe. With the baryon density determined by cosmic microwave background (CMB) observations, standard BBN predicts abundances of D, ${}^3\text{He}$, and ${}^4\text{He}$ that are in good accord with the observed abundances, however, there is a large discrepancy for ${}^7\text{Li}$. The observed ${}^7\text{Li}$ abundance appears to be depleted by a factor of about 3 when compared to the prediction of standard BBN in conjunction with CMB data. For recent reviews see Jedamzik & Pospelov (2009), Spite & Spite (2010), Steigman (2010), Fields (2011), Frebel & Norris (2011), Spite et al. (2012), and Coc et al. (2014).

${}^7\text{Li}$ is observed in the atmospheres of stars. It is best to observe old main-sequence and subgiant stars that are formed from primordial clouds because they are believed to preserve their lithium abundance. Very metal-poor stars are not sampled because they may not represent a lithium-rich star. ${}^7\text{Li}$ is a very fragile isotope that is destroyed at temperatures above 2.5×10^6 K. In stars that are too hot, convection within the star occurs close to the surface and leads to a mixing of the atmosphere and the hotter, deeper layers of the star, and destruction of ${}^7\text{Li}$, hence very hot stars are also not sampled. This has led to an emphasis on accurate modeling of the formation of Li. Ultimately, stellar ${}^7\text{Li}$ is thought to be preserved and provides the best representation of the primordial abundance in warm, metal-poor dwarf, or turnoff, stars (Spite et al. 2012). $A(\text{Li})$ determined from these stars is lower than expected. While some have argued for higher observed primordial ${}^7\text{Li}$ abundances (see e.g., Meléndez & Ramírez 2004; Meléndez et al. 2010; Howk et al. 2012), consistent with that expected from the CMB anisotropy data determination of the baryon density, here we focus on the more popular belief that standard BBN has a ${}^7\text{Li}$ problem and try to more carefully quantify this discrepancy than has previously been done.¹

The conventional assumption is that data errors have a Gaussian distribution when the data is of good enough quality.² Here we follow Chen et al. (2003)³ and consider the $A(\text{Li})$ data in this context. We construct the distribution of the errors of the lithium abundance, $A_i(\text{Li})_{-\sigma_i^l}^{+\sigma_i^u}$ (where $\sigma_i^{u(l)}$ is the 1 standard deviation upper (lower) error for the i^{th} abundance measurement), which is a plot of the number of measurements as a function of the number of standard deviations (N_σ) the measurement deviates from a central estimate $A(\text{Li})_{\text{CE}}$. Here

$$N_{\sigma_i} = \frac{A(\text{Li})_i - A(\text{Li})_{\text{CE}}}{\sigma_i^l} \quad (1)$$

¹There are many discussions of possible mechanisms that might be responsible for this discrepancy. See, for instance Jedamzik et al. (2006), Coc et al. (2007), Chakraborty et al. (2011), Fields (2011), Erkem et al. (2012), Cyburt et al. (2012), Ouyed (2013), and Kusakabe & Kawasaki (2014).

²For instance, this is used when determining constraints from CMB anisotropy data (see e.g., Ganga et al. 1997; Ratra et al. 1999; Chen et al. 2004; Bennett et al. 2013) and has been tested for such data (see e.g., Park et al. 2001; Ade et al. 2013).

³Chen et al. (2003) examine the error distribution of 461 Hubble constant measurements from Huchra’s list (many more than the 66 $A(\text{Li})$ measurements we will consider here). They discovered that the Hubble constant error distribution was very non-Gaussian and also confirmed the earlier Gott et al. (2001) median statistics estimate of the Hubble constant, more recently confirmed by Chen & Ratra (2011), $H_0 = 68 \pm 2.8$ km s^{−1} Mpc^{−1}. It is reassuring that many recent determinations of the Hubble constant agree with this median statistics estimate (see e.g., Calabrese et al. 2012; Sievers et al. 2013; Holanda et al. 2014; Wang et al. 2014).

when $A(\text{Li})_i < A(\text{Li})_{\text{CE}}$ and

$$N_{\sigma_i} = \frac{A(\text{Li})_i - A(\text{Li})_{\text{CE}}}{\sigma_i^u} \quad (2)$$

when $A(\text{Li})_i > A(\text{Li})_{\text{CE}}$. In this paper $A(\text{Li})_{\text{CE}}$ is the central estimate determined using either the weighted mean or the median technique. We find that the error distribution has larger tails than predicted by a Gaussian distribution. Spite & Spite (2010, Fig. 1), have already noted the non-Gaussianity of the ${}^7\text{Li}$ abundance error distribution. Here we present a quantitative analysis of this non-Gaussianity and fit the observed error distribution to various other commonly used distributions to determine which one provides a better fit.

In Section 2 we summarize the criteria used to compile the Spite et al. (2012) data. In this paper we are mostly concerned with the 66 (of 77) measurements that have error estimates. Section 3 describes our statistical analyses of the abundance data including finding central estimates using weighted mean and median statistics, analyzing the distribution of errors around the central estimates, and fitting several popular probability distribution functions to the observed error distribution. We conclude in Section 4.

2. Data selection

To ensure that the $A(\text{Li})$ data is representative of the primordial universe, Spite et al. (2012) select stars that have a metallicity that falls within the range $-2.8 \leq [\text{Fe}/\text{H}] \leq -2.0$. If the metallicity is larger, the star is too young to be considered and if the metallicity is smaller, the star fails to lie on the lithium plateau that can be seen in Spite et al. (2012). Next, they retain only those stars with shallower convection resulting in atmospheres that are good indicators of the primordial abundance of lithium. This shallow convection is seen in warm metal-poor stars with an effective temperature $T_{\text{eff}} \geq 5900$ K. These constraints result in a sample of 77 measurements. We do not consider two of the 77 measurements because they are upper bounds. In most of our statistical analyses we consider only 66 values of the remaining 75 (with an $A(\text{Li}) = 2.20 \pm 0.064$ (mean and 1σ error)) measurements that have error bars.⁴ These values are listed in Table 1.⁵ For these 66 measurements

⁴The remaining nine measurements have a quoted error of $\sigma = 0.01$, but this accounts only for that from the signal to noise ratio, and is not the full error, so we do not include these in our analyses here.

⁵The errors quoted in these references were found by adding in quadrature errors from stellar parameters and those from equivalent widths. Bonifacio et al. (2007) argue that the effective temperature error is larger than previously thought, and dominates the overall error, resulting in a constant error for all measurements. Given that we find the $A(\text{Li})$ error distribution is a non-Gaussian, to illustrate the possibility that this is the result of unaccounted-for systematic error, in the Appendix we repeat our analysis for the case with a

$A(\text{Li}) = 2.21 \pm 0.065$ (median and 1σ symmetrized error).

3. Analysis

3.1. Weighted mean and median statistics

We first compute central estimates using two different statistical techniques: weighted mean and median statistics.

The conventional weighted mean statistics has the advantage that a goodness-of-fit criterion can be obtained. The standard weighted mean formula (Podariu et al. 2001) is

$$A(\text{Li})_{\text{wm}} = \frac{\sum_{i=1}^N A(\text{Li})_i / \sigma_i^2}{\sum_{i=1}^N 1 / \sigma_i^2}, \quad (3)$$

where σ_i is the one standard deviation error of $i = 1, 2, \dots, N$ measurements.⁶ The weighted standard deviation is

$$\sigma_{\text{wm}} = \left(\sum_{i=1}^N 1 / \sigma_i^2 \right)^{-1/2}. \quad (4)$$

We can also determine a goodness of fit χ^2 by

$$\chi^2 = \frac{1}{N-1} \sum_{i=1}^N \frac{(A(\text{Li})_i - A(\text{Li})_{\text{wm}})^2}{\sigma_i^2}. \quad (5)$$

The number of standard deviations that χ deviates from unity is a measure of good-fit and is given by

$$N_\sigma = |\chi - 1| \sqrt{2(N-1)}. \quad (6)$$

Here $1/\sqrt{2(N-1)}$ is the expected error of χ . Hence N_σ represents the number of standard deviations χ deviates from unity. A large N_σ can be caused by correlations between measurements, systematic error, or invalidity of the Gaussian assumption.

constant error for all measurements. We thank F. Spite for helpful discussion on this matter.

⁶For measurements that have different upper and lower errors, we use the average of the two errors in the weighted mean formula.

Table 1: 66 Lithium Abundance Measurements from Spite et al. (2012).

Star Number/Name	A(Li) ^a	σ^{lb}	σ^{uc}	Reference
47480	2.17	0.061	0.061	Charbonnel & Primas (2005)
23344	2.13	0.026	0.026	
36513	2.15	0.094	0.078	
61361	2.25	0.063	0.027	
106468	2.24	0.025	0.024	
65206	2.07	0.057	0.048	
87467	2.25	0.067	0.057	
34630	2.12	0.052	0.049	
72461	2.22	0.066	0.059	
8572	2.24	0.027	0.026	
96115	2.22	0.028	0.021	
88827	2.31	0.052	0.048	
68321	2.15	0.033	0.031	
48152	2.25	0.029	0.027	
12529	2.22	0.024	0.046	
61545	2.15	0.075	0.062	
59109	2.27	0.057	0.059	
59376	2.11	0.019	0.020	
36430	2.35	0.042	0.040	
87693	2.20	0.041	0.045	
111372	2.28	0.086	0.096	
102337	2.30	0.062	0.053	Meléndez et al. (2010)
115704	2.15	0.038	0.041	
LP0815-0043	2.20	0.035	0.035	
BD-13 3442	2.18	0.035	0.035	
BD+03 0740	2.17	0.035	0.035	
BD+09 2190	2.13	0.035	0.035	
BD+24 1676	2.21	0.035	0.035	
LP0635-0014	2.28	0.035	0.035	
CD-35 14849	2.29	0.035	0.035	
BD-10 0388	2.21	0.035	0.035	
BD-04 3208	2.30	0.035	0.035	
HD 338529	2.23	0.035	0.035	
BD+02 3375	2.21	0.035	0.035	
HD 084937	2.26	0.035	0.035	
G011-044	2.30	0.035	0.035	
HD 24289	2.24	0.035	0.035	
BD+34 2476	2.23	0.035	0.035	
BD+42 3607	2.22	0.035	0.035	
BD+09 0352	2.21	0.035	0.035	
HD 19445	2.22	0.035	0.035	Aoki et al. (2009)
HD 74000	2.20	0.035	0.035	
+26 3578	2.28	0.070	0.070	Hosford et al. (2009)
042-003	2.26	0.070	0.070	
BD+03 ^o 740	2.13	0.074	0.074	
BD+09 ^o 2190	2.10	0.084	0.084	
BD-13 ^o 3442	2.15	0.057	0.057	
BD+26 ^o 2621	2.17	0.070	0.070	
BD+20 ^o 2030	2.07	0.068	0.068	
LP815-43	2.17	0.070	0.070	
BD+24 ^o 1676	2.16	0.009	0.009	
LP635-14	2.12	0.074	0.074	
CD-71 ^o 1234	2.20	0.035	0.035	
BD+26 ^o 3578	2.15	0.053	0.053	
CD-35 ^o 14849	2.24	0.025	0.025	
HD84937	2.17	0.066	0.066	
HD74000	2.05	0.083	0.083	
CS29518-020	2.13	0.090	0.090	Bonifacio et al. (2007)
CS30301-024	2.10	0.090	0.090	
CS29499-060	2.16	0.090	0.090	
CS31061-032	2.22	0.090	0.090	
BS17572-100	2.17	0.090	0.090	Sbordone et al. (2010)
CS22950-173	2.23	0.090	0.090	
CS29514-007	2.24	0.090	0.090	
G37-37	2.24	0.120	0.120	
G130-65	2.30	0.120	0.120	Schaeuble & King (2012)

^aFollowing the advice of M. Spite, for stars with both a main sequence and a sub-giant branch lithium abundance measurement, we list the average of the two values.

^bLower 1 σ error.

^cUpper 1 σ error.

The second statistical tool we use in analyzing the ${}^7\text{Li}$ measurements is median statistics. For a detailed description of median statistics see Gott et al. (2001).⁷ In using this method we assume that the measurements are statistically independent, and have no systematic error as a whole. As the number of measurements increase to infinity, the median will become a true value. This method has the advantage that it does not make use of the quoted errors. Consequentially this will result in a larger uncertainty than that of the weighted mean method.

If the measurements are statistically independent then there is a 50% chance of finding any value above or below the median. As described in Gott et al. (2001), the probability of the n^{th} measurement being higher or lower than the true median is

$$P_n = \frac{2^{-N} N!}{n!(N-n)!}. \quad (7)$$

With the use of weighted mean statistics we find a central estimate of $A(\text{Li})_{\text{wm}} = 2.20$ with a weighted error of $\sigma_{\text{wm}} = 4.43 \times 10^{-3}$. We also find $\chi^2 = 2.41$ and $N_\sigma = 6.28$; such a large value is cause for concern. Using median statistics we find a lithium abundance central estimate of $A(\text{Li})_{\text{med}} = 2.21$ with a 1σ range of $2.13 \leq A(\text{Li})_{\text{med}} \leq 2.26$, and a 2σ range of $2.05 \leq A(\text{Li})_{\text{med}} \leq 2.31$.⁸

Our central estimates are very similar to that of Spite et al. (2012). There they use a straight mean to estimate of $A(\text{Li}) = 2.20 \pm 0.064$ for the set of 75 measurements.

3.2. Error distribution and distribution functions

It is of interest to determine the error distribution of the ${}^7\text{Li}$ measurements. To do so, we plot the number of standard deviations each measurement deviates from the central estimate, as described in Chen et al. (2003). The formulae we use are in Eqs. (1) & (2) above. We use both the weighted mean and median statistics $A(\text{Li})_{\text{CE}}$ central estimates.

⁷For other applications see Chen & Ratra (2003), Hodge et al. (2008), Mamajek & Hillenbrand (2008), Bourne et al. (2011), Shafieloo et al. (2011), Croft & Dailey (2011), Andreon & Hurn (2012), Farooq et al. (2013), Crandall & Ratra (2014), and references therein.

⁸We also use median statistics to analyze the original set of 75 abundance values of Spite et al. (2012) since this method does not depend on the quoted errors. This results in a central estimate of $A(\text{Li})_{\text{med}} = 2.21$ with a 1σ range of $2.13 \leq A(\text{Li})_{\text{med}} \leq 2.26$, and a 2σ range of $2.07 \leq A(\text{Li})_{\text{med}} \leq 2.31$, reassuringly consistent with the values determined above.

Figure 1 shows the N_σ and $|N_\sigma|$ histograms using both central estimates.⁹

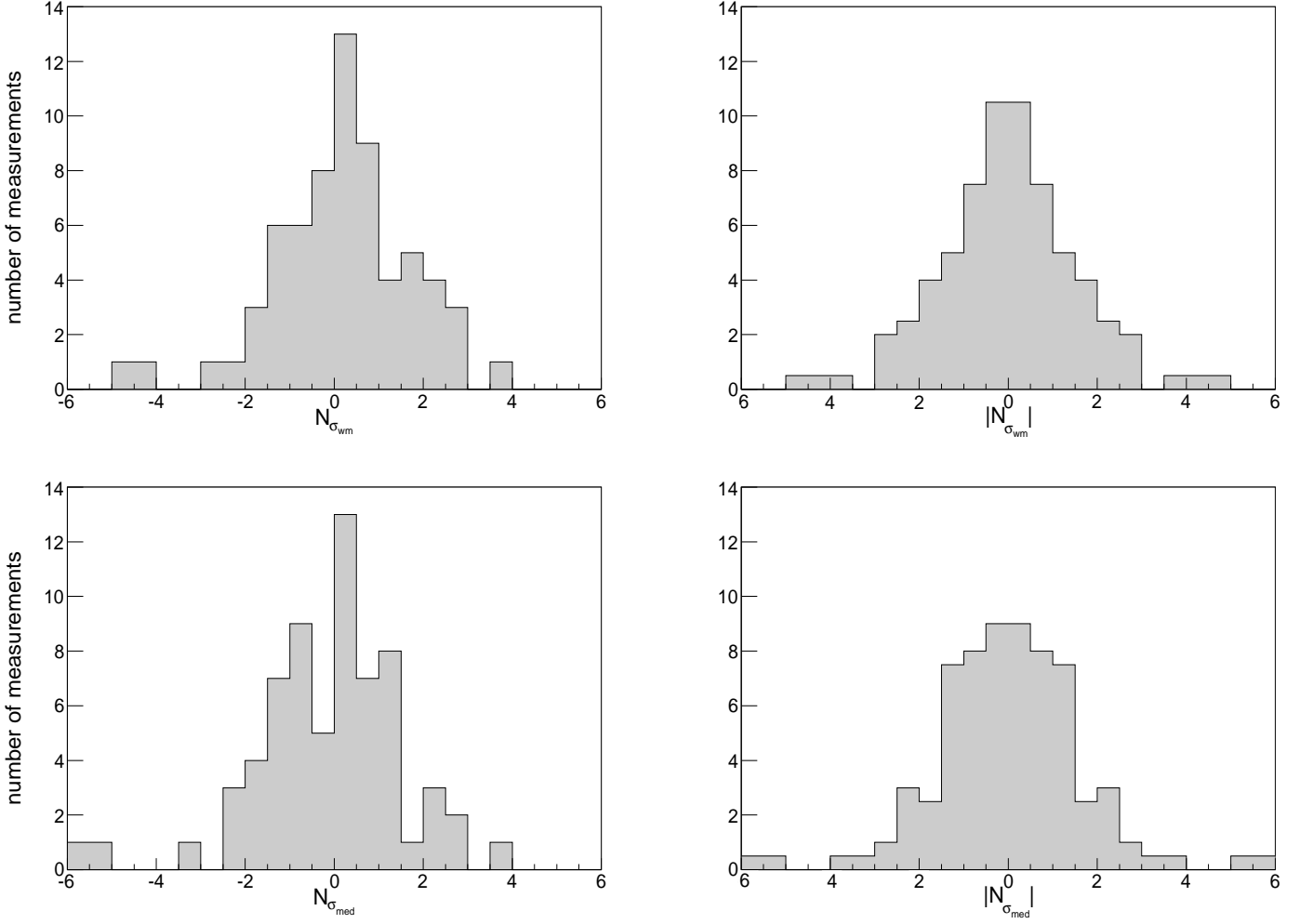


Fig. 1.— Histograms of the error distribution in half standard deviation bins. The top (bottom) row uses the weighted mean (median) of the 66 measurements as the central estimate. The left (right) column shows the signed (absolute) deviation. In the left column plots, positive (negative) N_σ represent a value that is greater (less) than the central estimate.

⁹The un-binned data used to derive the signed error distribution in the left column of Fig. 1 have a mean of $N_\sigma = 0.19$ (-0.14), median of $N_\sigma = 0.37$ (0.0), standard deviation $\sigma = 1.56$ (1.61), skewness -0.37 (-0.78) and a kurtosis of 0.61 (1.84) for the weighted mean (median) case.

For the weighted mean case, 68.3% of the signed error distribution falls within $-1.88 \leq N_\sigma \leq 1.15$ while 95.4% lies in the range of $-4.53 \leq N_\sigma \leq 2.03$ and the absolute magnitude of the error distribution have corresponding limits of $|N_\sigma| \leq 1.41$ and $|N_\sigma| \leq 3.0$ respectively. For the median statistics central estimate, 68.3% of the signed error distribution falls within $-1.75 \leq N_\sigma \leq 1.15$ while 95.4% lies within $-5.56 \leq N_\sigma \leq 2.25$ and the corresponding absolute magnitude limits are $|N_\sigma| \leq 1.31$ and $|N_\sigma| \leq 3.10$ respectively. Alternatively, when looking at the fraction of the data that falls within the $|N_\sigma| = 1$ and 2 ranges respectively, we obtain 54.5% and 81.8% for the weighted mean case and 51.5% and 81.8% for the median one. Although these fractions are large, they are not as large as for a Gaussian distribution. The error distribution of the 66 ${}^7\text{Li}$ abundance measurements used by Spite et al. (2012) is somewhat non-Gaussian. It is of interest to determine if a well-known non-Gaussian distribution function provide a better fit to the data.

To do this, we follow Chen et al. (2003) and bin our data so as to maximize the number of bins as well as the number of data points within each bin. This is best done by using the number of points per bin closest to the square root of the total number of measurements. We thus use 8 bins that are labeled by the integer $j = 1, 2, \dots, 8$, with each bin width allowed to vary to maintain about 8 measurements per bin. Adjusting the bin width, $\Delta|N_\sigma|_j$, ensures equal probability in each bin¹⁰ for the assumed distribution function. Therefore, for any of the assumed distributions, $P(|N_\sigma|)$, there are 8 bins that are expected to contain 8.25 data points.

We use the average of each bin to represent the bin as a whole and estimate a goodness of fit from a χ^2 analysis using

$$\chi^2 = \sum_{j=1}^8 \frac{[M(|N_\sigma|_j) - NP(|N_\sigma|_j)]^2}{NP(|N_\sigma|_j)}. \quad (8)$$

Here $M(|N_\sigma|)$ is the observed number of measurements in each bin and $N = 66$ is the total number of measurements. We use $P(|N_\sigma|)$, the assumed probability distribution function, to compute the expected number of measurements in bin j , $NP(|N_\sigma|_j)$. We continue on to calculate the reduced χ^2 , $\chi_\nu^2 = \chi^2/\nu$, where ν is the number of degrees of freedom (the number of bins, 8, minus the number of fitting parameters and the number of constraints). From χ_ν^2 and ν we are able to compute how well the probability distribution describes the spread of the measurements.¹¹ The values of χ_ν^2 and the corresponding probability for the probability

¹⁰From this point forward, we focus only on the symmetric absolute error distribution.

¹¹We assume the bins are uncorrelated in this computation of the probability, which is not necessarily true. Therefore, it is best to view the probability determined from χ_ν^2 as simply a qualitative indicator of goodness of fit and place a more quantitative emphasis on the value of χ_ν^2 .

distribution function for both the weighted mean and median analyses are compiled in Table 2.

Throughout this analysis we ensure that the constraint of the sum of the measurements being 66 is always satisfied. The degrees of freedom, ν , is equal to 7 (since there are 8 bins under consideration) when considering no additional free parameters. We fit the data to four probability distribution functions with each distribution centered at $|N_\sigma| = 0$ and only the absolute magnitude of the error distribution is used. In each case we also consider a corresponding probability distribution with a scale factor, S , that is used to vary the width of the distribution (consequently removing another degree of freedom) while minimizing χ^2 .

Although we have noted the non-Gaussianity of the error data, we will begin with the Gaussian probability distribution function where $|N_\sigma| = 1$ is synonymous with 1 standard deviation. The Gaussian distribution is

$$P(|N_\sigma|) = \frac{1}{\sqrt{2\pi}} \exp(-|N_\sigma|^2/2). \quad (9)$$

We also consider the function $P(|N_\sigma|/S)$ where we allow S to vary over 0.1–3, in steps of 0.1, and determine the value of S that minimizes χ^2 . When the scale factor, S , is not included (or equal to 1), we have $\nu = 7$ degrees of freedom. However, when S (an additional free parameter) is allowed to vary we have only $\nu = 6$ degrees of freedom. After normalizing both fits to unit area, shown in Fig. 2, we see that the measurement error distributions are poorly fitted by a Gaussian distribution (also see Table 2). Allowing the width of the Gaussian curve to vary to minimize χ^2 favors $S = 1.7$ for the weighted mean case. In this case 1 standard deviation is represented by $|N_\sigma| = 1.7$. This again points to the fact that the error distribution for the 66 measurements under consideration is non-Gaussian.¹²

¹²Although the error distributions of the lithium abundance measurements are non-Gaussian, this does not necessarily imply that the measurement errors themselves are non-Gaussian. Instead, it perhaps tells us something about the observers’ ability to correctly estimate systematic and statistical uncertainties.

Table 2. Goodness-of-Fit

Function	Weighted Mean				Median			
	Scale ^a	χ_ν^{2b}	ν^b	Probability(%) ^c	Scale ^a	χ_ν^{2b}	ν^b	Probability(%) ^c
Gaussian.....	1	65.8	7	< 0.1	1	101	7	< 0.1
Gaussian.....	1.7	10.9	6	< 0.1	1.8	11.5	6	< 0.1
Cauchy.....	1	6.70	7	< 0.1	1	7.31	7	< 0.1
Cauchy.....	1.6	5.54	6	< 0.1	1.6	6.00	6	< 0.1
$n = 8$ Student's t^d	1	25.3	6	< 0.1	1	30.4	6	< 0.1
$n = 8$ Student's t	2.6	2.04	5	6.9	2.8	2.16	5	5.5
Double Exponential.....	1	10.5	7	< 0.1	1	12.4	7	< 0.1
Double Exponential.....	1.4	8.76	6	< 0.1	1.5	9.94	6	< 0.1

^aFor a Gaussian distribution, $N_\sigma = 1$ corresponds to 1 standard deviation when the scale factor $S = 1$. For the other cases, the scale factor varies with the width of the distribution to allow χ^2 to be minimized.

^b χ_ν^2 is the χ^2 divided by the number of degrees of freedom ν .

^cThe probability that a random sample of data points drawn from the assumed distribution yields a value of χ_ν^2 greater than or equal to the observed value for ν degrees of freedom. This probability assumes that the bins are uncorrelated, which is not necessarily true. Therefore, the probabilities should only be viewed as qualitative indicators of goodness of fit.

^dWe find that for the Student's t distribution, the $n = 2$ and $S = 1$ case gives a smaller reduced $\chi_\nu^2 = 8.25$ (8.89) with a probability of < 0.1 (< 0.1) for the weighted mean (median) case. However, when allowing the scale factor S to vary, the $n = 8$ case has a lower reduced χ_ν^2 than the $n = 2$ case (also see footnote 11).

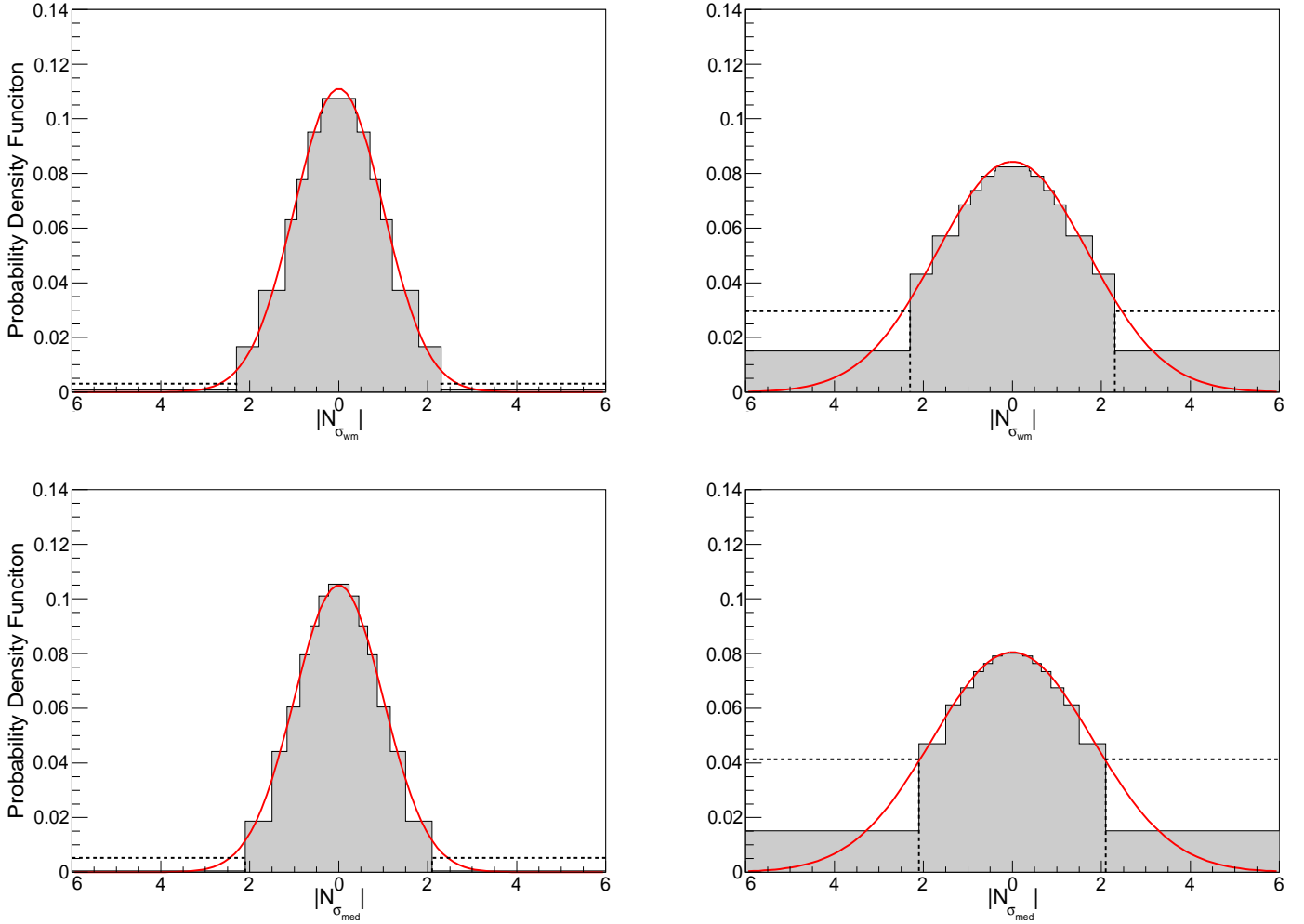


Fig. 2.— Best fit Gaussian probability density functions. The top left (right) plot represents the $|N_{\sigma_{wm}}|$ error distribution with scale factor $S = 1$ (1.7). The bottom left (right) plot represents the $|N_{\sigma_{med}}|$ error distribution with scale factor $S = 1$ (1.8). The dotted lines represent the predicted probability of the last bins brought in from $|N_{\sigma}| = \infty$ to $|N_{\sigma}| = 6.0$ with their heights adjusted to maintain the same probability.

Next, we turn to the Cauchy, or Lorentzian, distribution, which has an extended tail and is described by

$$P(|N_{\sigma}|) = \frac{1}{\pi} \frac{1}{1 + |N_{\sigma}|^2}. \quad (10)$$

Again, we also consider the case of $P(|N_\sigma|/S)$, where S is the scale factor that is allowed to vary while χ^2 is minimized. The best-fit Cauchy distributions for both weighted-mean and median central estimates are shown in Fig. 3, and numerical values are listed in Table 2. A Cauchy distribution with scale factor $S = 1$ is a poor fit, similar to the Gaussian distribution case, with a probability less than 0.1%. Although still not impressive, but a significant improvement nonetheless, the Cauchy distribution with a scale factor of $S = 1.6$ has a significantly larger probability but is still less than 0.1% although χ^2_ν is cut nearly in half. Furthermore, as listed in Table 3, it is apparent that the probability is much greater in the extended tails as 68.3% and 95.4% fall within $|N_\sigma| < 2.9$ and $|N_\sigma| < 22$, respectively, whereas the observed error distribution has the limits of $|N_\sigma| < 1.4$ and $|N_\sigma| < 3.0$. Therefore, it looks like a better fit will be one with broader tails than the Gaussian distribution but not as broad as that of the Cauchy distribution.

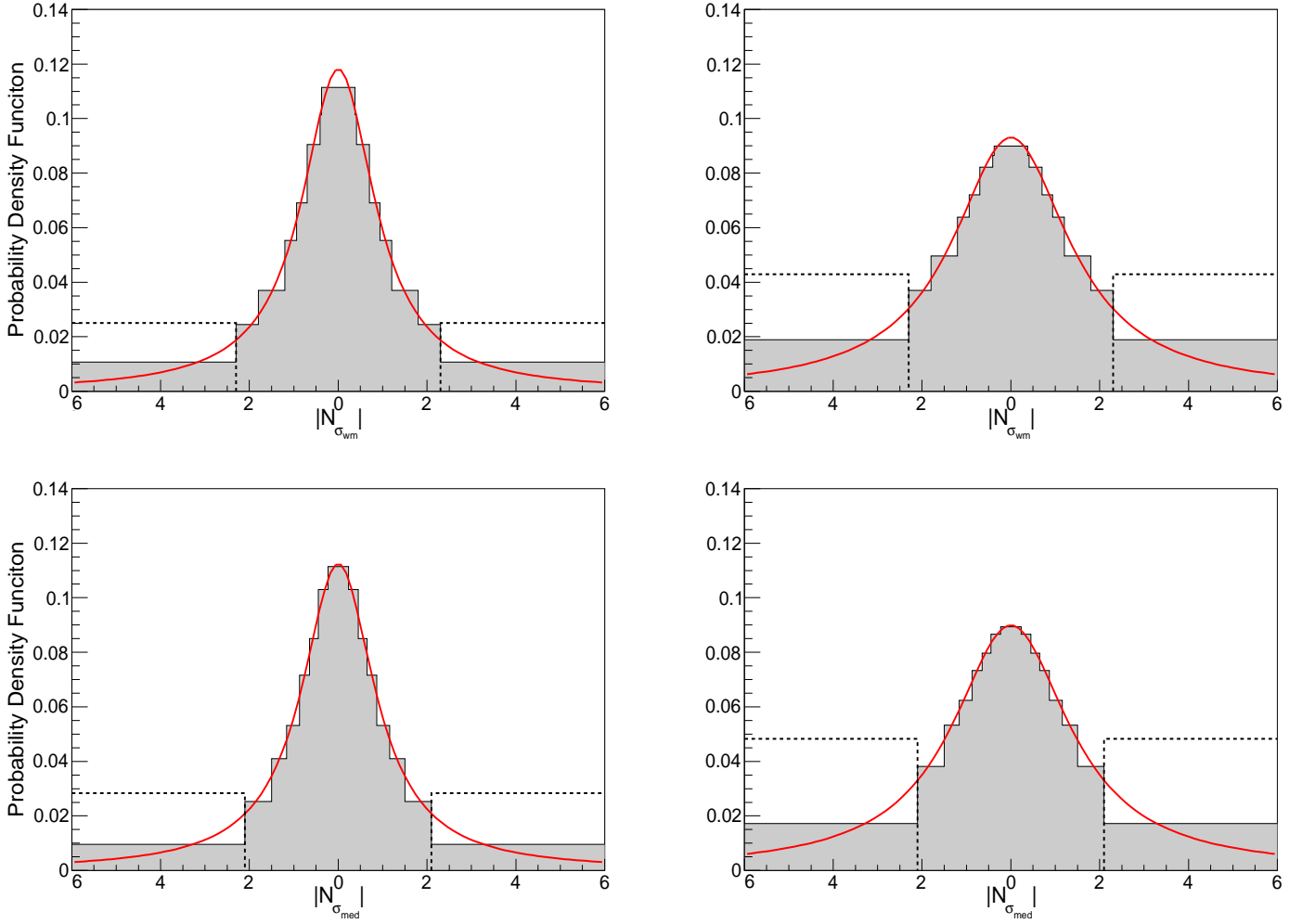


Fig. 3.— Best fit Cauchy probability density functions. The top left (right) plot represents the $|N_{\sigma_{wm}}|$ error distribution with scale factor $S = 1$ (1.6). The bottom left (right) plot represents the $|N_{\sigma_{med}}|$ error distribution with scale factor $S = 1$ (1.6). The dotted lines represent the predicted probability of the last bins brought in from $|N_{\sigma}| = \infty$ to $|N_{\sigma}| = 6.0$ with their heights adjusted to maintain the same probability.

This brings us to the consideration of the Student's t distribution which is described by the equation

$$P_n(|N_{\sigma}|) = \frac{\Gamma[(n+1)/2]}{\sqrt{\pi n} \Gamma(n/2)} \frac{1}{(1 + |N_{\sigma}|^2/n)^{(n+1)/2}}, \quad (11)$$

Table 3. $|N_\sigma|$ Limits^a

Function	Scale ^b	68.3% ^c	95.4% ^c
Gaussian.....	1	1.0	2.0
Gaussian.....	1.7	1.7	3.4
Gaussian.....	1.8	1.8	3.6
Cauchy.....	1	1.8	14
Cauchy.....	1.6	2.9	22
Cauchy.....	1.6	2.9	22
$n = 8$ Student's t	1	1.1	2.4
$n = 8$ Student's t	2.6	2.8	6.1
$n = 8$ Student's t	2.8	3.0	6.6
Double Exponential.....	1	1.2	3.1
Double Exponential.....	1.4	1.6	4.3
Double Exponential.....	1.5	1.7	4.6
Observed Weighted Mean		1.4	3.0
Observed Median.....		1.3	3.1

^aFor each set of named distribution functions, the first line is for the standard distribution and the second and third lines are for the distributions that best fit the error distribution constructed using the weighted mean and median central estimate respectively.

^bFor a Gaussian distribution, $N_\sigma = 1$ corresponds to 1 standard deviation when the scale factor is $S = 1$. For the other functions, unless $S = 1$, the scale factor varies with the width of the distribution to allow χ^2 to be minimized.

^cThe $|N_\sigma|$ limits that contain 68.3% and 95.4% of the probability.

where Γ is the gamma function and n is a positive integer (which consequently eliminates another degree of freedom; so now when not varying the scale factor $\nu = 6$). As usual, we also consider the case of $P_n(|N_\sigma|/S)$, where S is allowed to vary in such a way (from 0.1–3) to allow χ^2 to be minimized. We consider Student’s t distribution because at $n = 1$ Student’s t distribution is synonymous with the Cauchy distribution, and as $n \rightarrow \infty$ Student’s t distribution approaches a Gaussian distribution. Therefore, Student’s t distribution will have broader tails than the Gaussian distribution and narrower tails than the Cauchy distribution when $1 < n < \infty$, along the lines of what the A(Li) error distributions seem to demand.

We have fitted Student’s t distribution to the error distributions of A(Li) while allowing n to vary over integer values between 2 and 30 as χ_ν^2 is minimized (see Fig. 4). When considering the corresponding $P_n(|N_\sigma|/S)$ (in which case $\nu = 5$), we allow n to be any integer value between 2 and 30 while simultaneously allowing S to adjust over 0.1 – 3 for the best χ_ν^2 .¹³ In this case the best fit occurs when $n = 8$ and $S = 2.6$ ¹⁴ where χ^2 is minimized, resulting in the highest probability of 6.9% (Table 2). With Student’s t fit, only 29% of the data falls within $|N_\sigma| < 1$ and 68.3% of the data falls within $|N_\sigma| < 2.8$ as expressed in Table 3 and Table 4.

¹³When allowing n to vary, a pattern began to form that resulted in a progressively better fit for every even value of n . As we looked for the smallest χ_ν^2 for each value of n , S had to be raised exponentially (we exceeded our upper bound of 3 on S). For $n = 10$ and $S = 3.1$ there was a reduced χ^2 probability of $\sim 29\%$, for $n = 12$ and $S = 3.8$ the probability was $\sim 61\%$, for $n = 14$ and $S = 4.7$ the probability was $\sim 86\%$, and for $n = 20$, we must have approached an asymptote because for $S > 1000$ χ_ν^2 showed very gradual change, while still minimizing, resulting in a probability of $\sim 99.9\%$.

¹⁴This, of course, only applies to our arbitrary limits of $0.1 \leq S \leq 3.0$, which we will consider our “best fit” probability distribution from this point forward.

Table 4. Expected Fractions^a

Function	Scale ^b	$ N_\sigma \leq 1^c$	$ N_\sigma \leq 2^c$
Gaussian.....	1	0.68	0.95
Gaussian.....	1.7	0.44	0.76
Gaussian.....	1.8	0.42	0.73
Cauchy.....	1	0.50	0.71
Cauchy.....	1.6	0.36	0.57
Cauchy.....	1.6	0.36	0.57
$n = 8$ Student's t	1	0.65	0.92
$n = 8$ Student's t	2.6	0.29	0.54
$n = 8$ Student's t	2.8	0.27	0.50
Double Exponential.....	1	0.63	0.87
Double Exponential.....	1.4	0.51	0.76
Double Exponential.....	1.5	0.49	0.74
Observed Weighted Mean		0.55	0.82
Observed Median.....		0.52	0.82

^aFor each set of named distribution functions, the first line is for the standard distribution and the second and third lines are for the distributions that best fit the error distribution constructed using the weighted mean and median central estimate respectively.

^bFor a Gaussian distribution, $N_\sigma = 1$ corresponds to 1 standard deviation when the scale factor is $S = 1$. For the other functions, unless $S = 1$, the scale factor varies with the width of the distribution to allow χ^2 to be minimized.

^cThe fraction of the area that lies within $|N_\sigma| = 1$ and $|N_\sigma| = 2$.

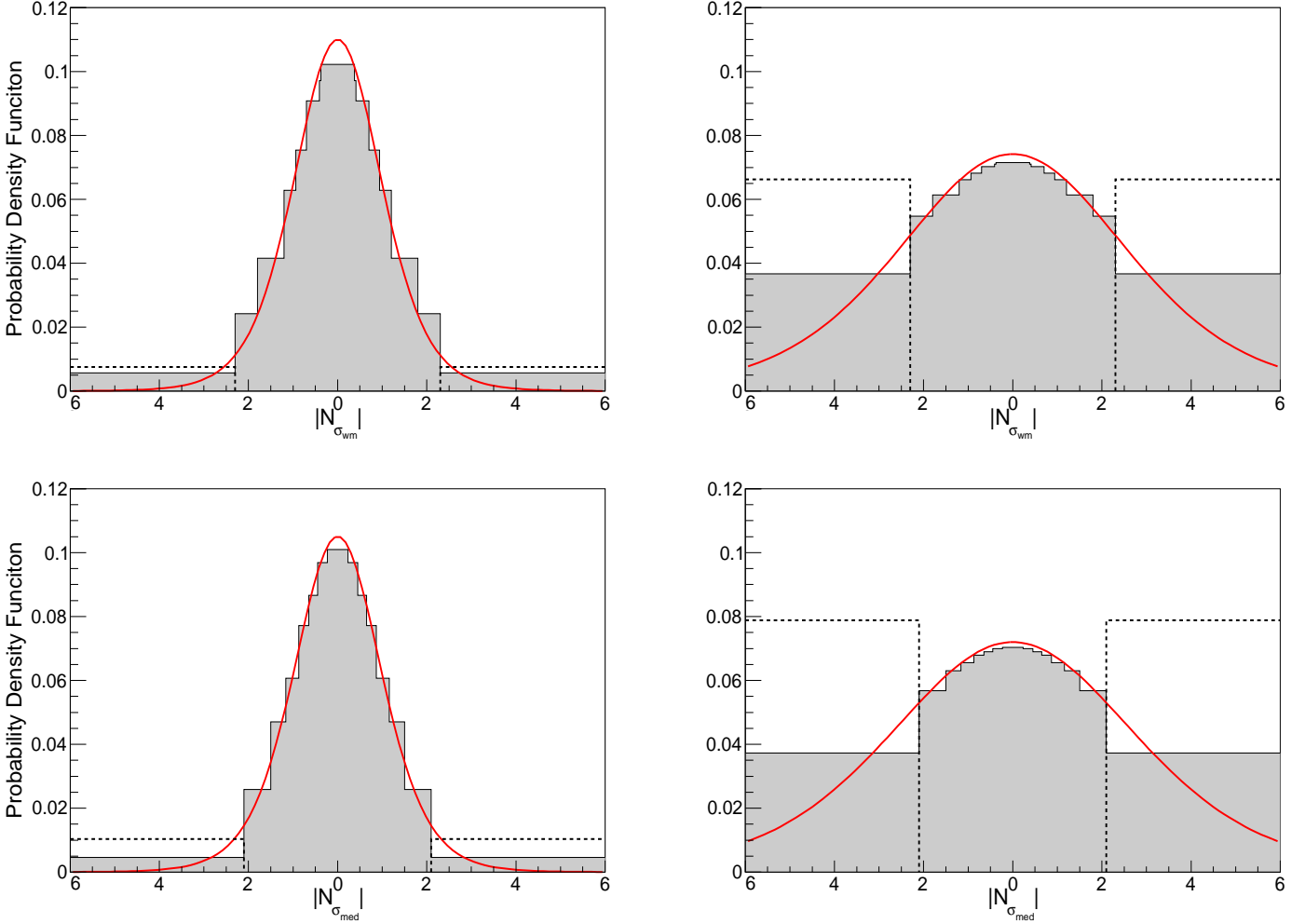


Fig. 4.— Best fit Student's t probability density functions. The top left (right) plot represents the $|N_{\sigma_{wm}}|$ error distribution with scale factor $S = 1$ (2.6) and $n = 8$. The bottom left (right) plot represents the $|N_{\sigma_{med}}|$ error distribution with scale factor $S = 1$ (2.8) and $n = 8$. The dotted lines represent the predicted probability of the last bins brought in from $|N_{\sigma}| = \infty$ to $|N_{\sigma}| = 6.0$ with their heights adjusted to maintain the same probability.

Finally, we consider the double exponential, or Laplace, distribution,

$$P(|N_{\sigma}|) = \frac{1}{2}e^{-|N_{\sigma}|}. \quad (12)$$

The double exponential distribution falls off more rapidly than the Cauchy distribution, but not as quickly as the Gaussian distribution. When considering $P_n(|N_{\sigma}|/S)$ we found the best

fit was when $S = 1.4$, resulting in 68.3% of the data falling within $|N_\sigma| = 1.6$ and 95.4% of the data within $|N_\sigma| = 4.3$ which is shown numerically in Table 3 and visually in Figure 5.

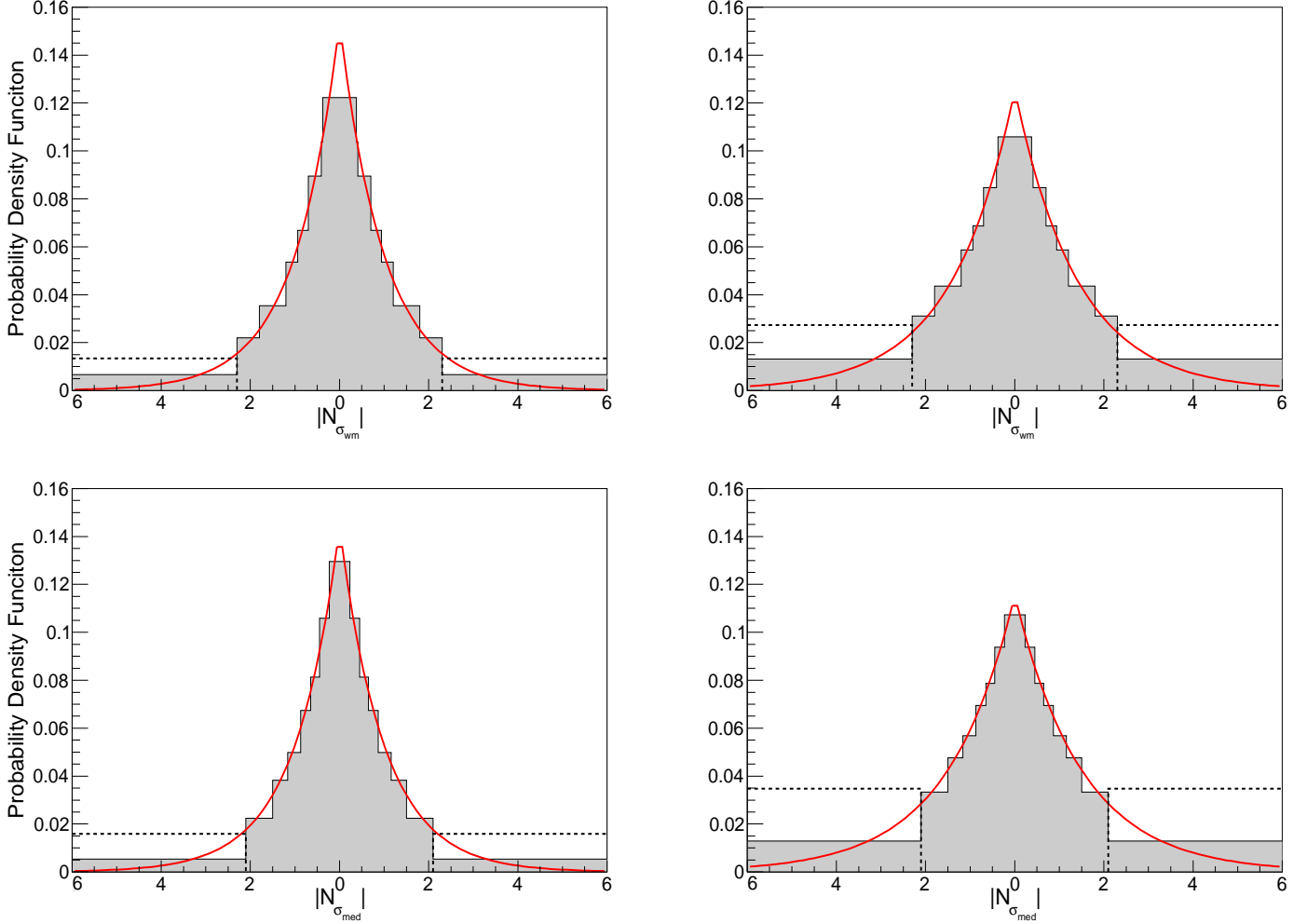


Fig. 5.— Best fit double exponential probability density functions. The top left (right) plot represents the $|N_{\sigma_{wm}}|$ error distribution with scale factor $S = 1$ (1.4). The bottom left plot represents the $|N_{\sigma_{med}}|$ error distribution with scale factor $S = 1$ (1.5). The dotted lines represent the predicted probability of the last bins brought in from $|N_\sigma| = \infty$ to $|N_\sigma| = 6.0$ with their heights adjusted to maintain the same probability.

4. Conclusion

We have used a compilation of 66 ${}^7\text{Li}$ abundance measurements from Spite et al. (2012) to attempt to gain a better understanding of the lithium problem. Confirming the observation of Spite & Spite (2010), we find that the $A(\text{Li})$ error distribution is non-Gaussian. As noted above, this perhaps tells us something about the observers’ ability to estimate systematic and statistical uncertainties.¹⁵ This could also be an indication that a definite resolution might need to wait for more and higher-quality data. However, here we speculate a bit about the statistical significance of the Li problem.

To determine the statistical significance of the discrepancy, we first assume Gaussianity and find the difference between the mean of the *Planck* data predicted value $A(\text{Li}) = 2.69$ (Coc et al. 2014) and our median value $A(\text{Li}) = 2.21$. We divide this difference by the quadrature sum of our error ($\sigma = 0.065$) and that from Coc et al. (2014) ($\sigma = 0.034$). This results in a 6.5σ discrepancy. To account for the non-Gaussianity, we simply multiply our $\sigma = 0.065$ error by 1.4 (Table 3, second to last line) in the quadrature sum, resulting in a 4.9σ discrepancy.

To attempt to characterize the $A(\text{Li})$ error distribution, we fit various popular probability distribution functions to it. We find that the observed error distribution has larger probability in the tails than a Gaussian distribution, but less than a Cauchy distribution. While allowing the scale factor to vary over the range $0.1 \leq S \leq 3$, the error distribution is best fit by an $n = 8$ Student’s t distribution, although better fits can be found for larger n and S . We have not followed up on this in detail since this is unlikely to be of much physical significance.

In conclusion, while it would be good to have more and higher-quality $A(\text{Li})$ data that results in a Gaussian error distribution so as to be able to draw a definite conclusion, it seems fair to conclude that the non-Gaussianity of the current data cannot fully resolve the Li problem.

We thank M. Spite for providing us with helpful insight and the data compiled in Spite et al. (2012). We are grateful to F. Spite for very useful advice. This work was supported in part by DOE Grant No. DEFG 03-99EP41093, and NSF Grant Nos. AST-1109275 and PHY-1157044.

¹⁵We examine an illustrative example in the Appendix.

Appendix

Bonifacio et al. (2007) have argued that the effective temperature error is larger than previously thought. If this is so then it could dominate the error, resulting in the same error for each A(Li) measurement. To illustrate the effect of such a potential error, we repeat our analysis with a constant, optimistic, $\sigma = 0.06$.¹⁶ For the weighted mean case 68.3% of the signed error distribution falls within $-1.48 \leq N_\sigma \leq 0.80$ while 95.4% lies in the range of $-2.47 \leq N_\sigma \leq 1.39$ and the absolute magnitude of the error distribution have corresponding limits of $|N_\sigma| \leq 1.15$ and $|N_\sigma| \leq 2.13$ respectively. For the median statistics central estimate 68.3% of the signed error distribution falls within $-1.37 \leq N_\sigma \leq 0.83$ while 95.4% lies within $-2.39 \leq N_\sigma \leq 1.60$ and the corresponding absolute magnitude limits are $|N_\sigma| \leq 1.16$ and $|N_\sigma| \leq 2.32$ respectively. Alternatively, when looking at the fraction of the data that falls within the $|N_\sigma| = 1$ and 2 ranges respectively, we obtain 62.7% and 94.7% for the weighted mean case and 65.3% and 95.4% for the median one. As one might expect, these fractions are more Gaussian than values found in the analysis in the body of our paper. The N_σ histograms are shown in Fig. 6.

¹⁶We also used the more conservative $\sigma = 0.09$ of Bonifacio et al. (2007) and reached similar conclusions.

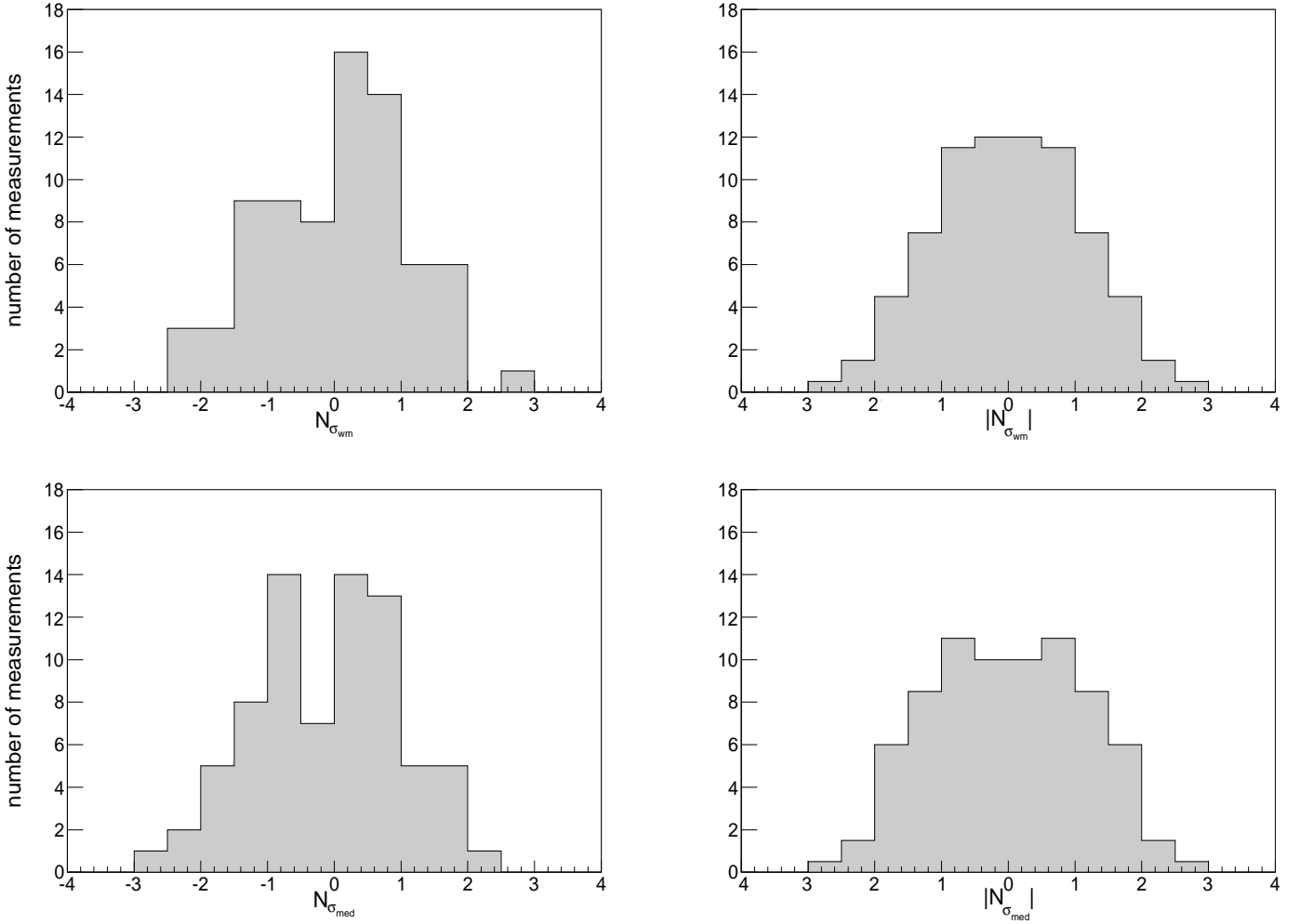


Fig. 6.— Histograms of the error distribution with $\sigma = 0.06$ A(Li) values in half standard deviation bins. The top (bottom) row uses the weighted mean (median) of the 66 measurements as the central estimate. The left (right) column shows the signed (absolute) deviation. In the left column plots, positive (negative) N_{σ} represent a value that is greater (less) than the central estimate.

REFERENCES

Ade, P. A. R., et al., 2013, arXiv:1303.5084v1 [astro-ph.CO]

- Andreon, S., & Hurn, M. A., 2012, arXiv:1210.6232v1 [astro-ph.IM]
- Aoki, W., et al., 2009, ApJ, 698, 1803
- Bennett, C. L., et al. 2013, ApJS, 208, 20
- Bonifacio, P., et al., 2007, A&A, 462, 851
- Bourne, N., et al., 2010, MNRAS, 410, 1155
- Calabrese, E., Archidiacono, M., Melchiorri, A., & Ratra, B., 2012, Phys. Rev. D, 86, 043520
- Chakraborty, N., Fields, B. A., & Olive, K. A., 2011, Phys. Rev. D, 83, 063006
- Charbonnel, C., & Primas, F., 2005, A&A, 442, 961
- Chen, G., Gott, R., & Ratra, B., 2003, PASP, 115, 1269
- Chen, G., Mukherjee, P., Kahniashvili, T., Ratra, B., & Wang, Y., 2004, ApJ, 611, 655
- Chen, G., & Ratra, B., 2003, PASP, 115, 1143
- Chen, G., & Ratra, B., 2011, PASP, 123, 1127
- Coc, A., Nunes, N. J., Olive K. A., Uzan J. P., & Vangioni, E., 2007, Phys. Rev. D, 76, 023511
- Coc, A., Uzan, J., & Vangioni, E., 2014, arXiv:1403.6694v1 [astro-ph.CO]
- Crandall, S., & Ratra, B., 2014, Phys. Lett. B, 732, 330
- Croft, R. A. C., & Dailey, M., 2011, arXiv:1112.3108v1 [astro-ph.CO]
- Cyburt, R. H., et al., 2012, JCAP, 1212, 037
- Erkem, O., Sikivie, P., Tam H., & Yang, Q., 2012, Phys. Rev. Lett., 108, 061304
- Farooq, O., Crandall, S., & Ratra, B., 2013, Phys. Lett. B, 726, 72
- Fields, B. D., 2011, Ann. Rev. Nucl. Part. Sci., 61, 47
- Frebel, A., & Norris, J. E., 2011, arXiv:1102.1748v2 [astro-ph.GA]
- Ganga, K., Ratra, B., Gundersen, J. O., & Sugiyama, N., 1997, ApJ, 484, 7
- Gott, J. R., Vogeley, M. S., Podariu, S., & Ratra, B., 2001, ApJ, 549, 1

- Holanda, R. F. L., Busti, V. C., & da Silva, G. P., 2014, arXiv:1404.4418v2 [astro-ph.CO]
- Hosford, A., Ryan, S. G., García Pérez, A. E., Norris, J. E., & Olive, K. A., 2009, A&A, 493, 601
- Hodge, J. A., Becker, R. H., White, R. L., & de Vries, W. H., 2008, AJ, 136, 1097
- Howk, J. C., Lehner, N., Fields, B. D., & Mathews, G. J., 2012, Nature, 489, 121
- Jedamzik, K., Choi, K. Y., Roszkowski, L., & de Austri, R. R., 2006, JCAP, 0607, 007
- Jedamzik, K. & Pospelov, M., 2009, New J. Phys., 11, 105028
- Kusakabe, M. & Kawasaki, M., 2014, arXiv:1404.3485 [astro-ph.CO]
- Mamajek, E. E. & Hillenbrand, L. A., 2008, ApJ, 687, 1264
- Meléndez, J., Casagrande, L., Ramírez, I., Asplund, M., & Schuster, W. J., 2010, A&A, 515, L3
- Meléndez, J. & Ramírez, I., 2004, ApJ, 615, L33
- Ouyed, R., 2013, arXiv:1304.3715v2 [astro-ph.HE]
- Park, C. G., Park, C., Ratra, B., & Tegmark, M., 2001, ApJ, 556, 582
- Podariu, S., Souradeep, T., Gott, J. R., Ratra, B., & Vogeley, M. S., 2001, ApJ, 559, 9
- Ratra, B., et al. 1999, ApJ, 517, 549
- Sbordone, L., et al., 2010, A&A, 522, A26
- Schaeuble, M. & King, J.R., 2012, PASP, 124, 164
- Shafieloo, A., Clifton, T., & Ferreira, P., 2011, JCAP, 1108, 017
- Sievers, J. L., et al. 2013, JCAP, 1310, 060
- Spite, M., & Spite, F., 2010, in Light Elements of the Universe, ed. C. Charbonnel, M. Tosi, F. Primas, C. Chiappini (Cambridge, UK: Cambridge University Press), 201
- Spite, M., Spite, F., & Bonifacio, P., 2012, Mem. S.A.It. Suppl., 22, 9
- Steigman, G., 2010, arXiv:1008.4765v2 [astro-ph.CO]
- Wang, Y., Wands, D., Zhao G. -B., & Xu, L., 2014, Phys. Rev. D, 90, 023502

